AD-A264 278

DCUMENTATION PAGE

Form Approved
OMB No 0704-0188

(2)

2. REPORT DATE	3. REPORT TYPE AND DATES COVERED
April 1993	Final Report 6/1/90 - 5/31/91

4. TITLE AND SUBTITLE
Biotechnology Symposium

5. FUNDING NUMBERS
61102F 2303 B2

6. AUTHOR(S)
Barbara C. Woolsey

7. PERFORMING ORGANIZATION NAME(S) AND ADDRESS(ES)
American Society for Composites
211 North Broad Street
Fairborn, OH 45324-4932

8. PERFORMING ORGANIZATION REPORT NUMBER
AFOSR-TR- [illegible]9

9. SPONSORING/MONITORING AGENCY NAME(S) AND ADDRESS(ES)
AFOSR/NC
Building 410, Bolling AFB DC
20332-6448

10. SPONSORING/MONITORING AGENCY REPORT NUMBER
AFOSR-90-0293

11. SUPPLEMENTARY NOTES

12a. DISTRIBUTION/AVAILABILITY STATEMENT
APPROVED FOR PUBLIC RELEASE; DISTRIBUTION IS UNLIMITED.

12b. DISTRIBUTION CODE

13. ABSTRACT (Maximum 200 words)

As part of a meeting of the American Society of Composites, 10-13 Jun 1990, an Air Force supported session on "Biotechnology and Composite Materials" was held. The titles of the presentations in this session were as follows: "An Overview of Three Biotechnology Areas for the Development of Advanced Composite Materials and Structures"; "Seashells as a Natural Model to Study Laminated Composites"; "Recombinant Spider Silk Proteins for Composite Fibers"; "Treatment of Graphite Fiber Surfaces with Gram-Negative Aerobic Bacteria"; "Modeling the Effects of Aging on Bone Properties Using Composite Material Micromechanics".

14. SUBJECT TERMS

15. NUMBER OF PAGES
43

16. PRICE CODE

17. SECURITY CLASSIFICATION OF REPORT	18. SECURITY CLASSIFICATION OF THIS PAGE	19. SECURITY CLASSIFICATION OF ABSTRACT	20. LIMITATION OF ABSTRACT
UNCLASSIFIED	UNCLASSIFIED	UNCLASSIFIED	

SESSION 2A

Biotechnology and Composite Materials

Co-Chair: R. Narayan, Michigan Biotechnology Institute
Co-Chair: R. C. Schiavone, University of Dayton Research Institute

An Overview of Three Biotechnology Areas for the Development of Advanced Composite Materials and Structures

S. L. GUNDERSON,[1] R. NARAYAN[2] AND R. C. SCHIAVONE[1]

ABSTRACT

Biotechnology, in general terms, is the science and engineering of using living organisms for making useful products such as pharmaceuticals, foods, fuels, chemicals, materials or in waste treatment processes and clinical and chemical analyses. It encompases the prosaic form of using yeast cells to make bread and alcohol to the more exciting world of using recombinant DNA technology for producing critically important pharmaceuticals such as human insulin [1]. However, the use of biotechnology in composite materials has just recently been recognized as a potential contributor to the aerospace materials and structures industry. Examples of various biotechnology fields of research that may offer potential applications are: biodegradation, biomimetics, biomining, bio-optics/bioelectronics biosynthesis and bioprocessing. This paper will examine research in the areas of biomimetics, biosynthesis and bioprocessing.

INTRODUCTION

Biomimetics involves the study of natural systems and structures for novel designs and material utilization that could improve the versatility and performance capabilities of synthetic materials and structures. An example is the study of natural composites for unique material organization that can be translated to synthetic composites for improved properties.

---

[1]University of Dayton Research Institute, Dayton, OH 45469-0001
[2]Michigan Biotechnology Institute, 3900 Collins Rd., Lansing, MI 48910

Biosynthesis involves the use of living organisms for the production of chemicals and materials such as composite resins or resin precursors. It is possible that biosysnthesis will allow production of current materials at lower costs with greater efficiency as well as produce new materials which are unavailable through synthetic chemistry alone [2].

Bioprocessing involves the processing of biologically derived polymers into composite structures. An example is the use of natural polymers such as chitin, lignicellulosics or genetically engineered protein polymer precursors into useful composite materials and structures.

BIOMIMETICS

Nature utilizes relatively weak, pliant and thermally unstable constituent materials to create composite structures that are strong, stiff, tough, lightweight and resistant to many chemicals [3,4]. The constituents used by nature include: proteins, polysaccharides, minerals, waxes and lipids, and water [5]. Materials and structures such as wood, shell, bone, insect exoskeleton, skin and tendon are excellent examples of natural composites. As can be seen, nature provides materials with a range of properties from very soft and pliant to those of high strength and stiffness while using many of the same starting materials. A brief description of the materials and structures of wood, insect exoskeleton, mollusc shell and bone will be presented along with possible applications to synthetic materials and structures.

WOOD

The materials which make up the structure of wood are water, a fibrous cellulose and a combination of amorphous hemicelluloses and lignin which makes up the matrix. Cellulose microfibrils, having diameters of approximately 10 to 25 nm, are embedded in the hemicellulos-lignin matrix and arranged to form concentrically layered cylinders called cells [5]. The wood cell wall is divided into the primary wall, containing a loose irregular network of microfibrills, and the secondary wall, which is composed of three seperate and distinct layers (S1, S2, S3) each containing various helical fiber architectures. The central core of the wood cell is called the lumen and may either be hollow or filled with fluid and nutrients. Wood cells, measuring approximately 2 mm long and 50 microns in diameter, are grouped together and oriented along the long axis of the structure [6] (Fig. 1).

Since wood and wood cells perform better in tension than compression, various "tricks" are used to aid performance. These include the cellular structure of the wood cells and the use of water to provide internal hydrostatic pressure. Also, areas subjected to large compressive forces, such as the lower half of limb joints and the outer portion of trunks, are prestressed in tension to necessitate increased compressive loads for instigating failure. Another interesting trick is the use of reaction wood which is a group of specialized wood cells created to resist either tensile or compressive forces. Compression wood cells are circular in cross section and have thicker layers than normal wood cells. The microfibril angle is greater than normal and the matrix content is increased while the microfiber volume is decreased. Tension wood cells are irregularly shaped and packed tightly together. Also, the microfiber volume is increased with the microfibril angle more closely aligned to the long axis of the cell [7].

Application areas of wood to man-made composites could include its cellular microstructure for providing information to the design of novel fibers and structures. The structure of the wood cell itself; the varying cell walls, microfibril orientation and overall structure; could be applied to fiber development and the structures of cylinders, trusses and stiffeners. Also, the use of hydrostatic, or internal, pressure could possibly be applied in the form of an incompressible material to help resist compressive loads. An aplication has already been patented by Chaplin et al. [8] where a series of composite cylinders, panels and sandwich structures were constructed based on the helical winding angle of cellulose fibrills in the wood cell.

INSECT EXOSKELETON

The principle materials found in insect exoskeletons are chitin (a high molecular weight sugar), proteins, water, waxes and lipids. Chitin molecules form long chains that combine to form microfibrils with diameters of about 3 nm. In some cases, these microfibrils combine to form fibers that have diameters from about 2-7 microns. In either case, the microfibers or fibers are unidirectionally embedded in the fibrous protein matrix forming a ply. The unidirectional plies are stacked in various layup orientations ranging from unidirectional to random to a dual helical pattern and forms the section known as the procuticle (Fig. 2). The protein matrix in the procuticle is soft upon fiber embedding but may undergo a hardening process called sclerotisation. The exoskeleton may be composed of completely sclerotised (exocuticle), unsclerotised

(endocuticle) or a combination of both matrix states [9]. Waxes and lipids are found in the outer epicuticle layer and act as an environmental barrier similar to the coatings used on man-made composite structures.

The exoskeleton is strong, stiff, tough, and shows very little fiber pull-out on the fracture surface. Much of this may be attributed to the unique interface between the chitin fibers and protein matrix. With the fibrous matrix and microfibril branching, an interface may be formed by the insect that is superior to those found in man-made composites. Another unique design discovered in the bessbeetle procuticle was a network of microfiber bridging between adjacent fibers and plies [10]. This microfiber bridging may be utilized for improved load transfer and to increase the shear strength and damage tolerance of the structure.

Possible areas of interest could be the fiber morphology, size, shape, surface characteristics and distribution; fiber orientation; fiber/matrix interface; matrix gradients; and sensor utilization. These areas could be applied to hybrid composites, ultra-lightweight materials and structures, and smart materials and structures.

BONE

The principal materials making up bone are collagen, calcium phosphate and water. Collagen, used as the matrix, is found in the form of small microfibrils. Reinforcement is provided by calcium phospate as crystalized hydroxyapatite plates or needles having cross sectional areas of approximately 100 square nm. The collagen microfibrils are first laid down as triple helically wound concentric lamella. The mineral is then crystalized as hydroxyapatite and deposited on and in between the collagen fiber network forming the microscopic structure called an osteon. These osteons are then grouped together to form the final bone structure, similar to the grouping of wood cells (Fig. 3). The weight percents of collagen and hydroxyapatite are 28% and 60% respectively however their volumes are equal [11].

Bone utilizes such unique designs as a cellular microstructure (osteons), a fibrous matrix and internal hydrostatic pressure. Also, microfiber bridging has been observed between collagen fiber lamella within osteons [12]. Analysis performed in these areas may aid in the improvement of compression properties and development of molecular composites. Ceramic matrix composites may also benefit from insight to novel methods of material usage and organization.

MOLLUSC SHELL

Most mollusc shell material is composed of crystalline calcite or aragonite (forms of calcium carbonte) and a protein film which is utilized as the binder in varying amounts from 0.1% to 5% by weight. The primary types of shell structure are nacre, crossed lamellar, foliated and prismatic. Nacre is the strongest and toughest of the shell types and will be the only one described here. Nacre is constructed of aragonite crystals which are aranged in sheets and stacked to form laths. These very thin laths (approx. 0.5 microns) are laid parallel to the shell surface and bound together by a protein film forming a lamellate structure (Fig. 4). The orientation of aragonite sheets in adjacent laths is varied so as to deter the propogation of cracks through the thickness of the shell [13].

The principal type of loading observed by shells is impact. Therefore, novel toughening mechanisms are developed using unique mineral orientations and fiber/plate pullout mechanisms. Other toughening mechanisms present include crack branching, crack blunting and crack bridging by the matrix [14]. These toughening devices should be of interest to those working with ceramic- or metal-matrix composites. Also, the location dependent crystal size and geometry observed in the shell structure and the method by which they are grown could be other areas of application.

BIOSYNTHESIS

PROTEIN COMPOSITES

Nature has been able to formulate protein polymers with extraordinary mechanical properties such as the toughness of silk and the elasticity and resilience of mammalian elastin. Therefore, great interest exists in producing these polymers in sufficient quantities using genetic engineering approaches which could offer the potential of property enhancement at a lower cost over conventional means.

Silk made from the caterpillar, *Bombyx mori*, has outstanding mechanical and good thermal properties. The *Bombyx mori* synthesises the components of silk inside its body and extrudes them in the form of a silk fibre which it spins into a cocoon. The silk fibre consists of twin filaments of the protein fibroin which are glued together by the protein sericin.

Many other insects produce silk, most notably spiders. Spider silks are proteins with molecular weights approaching 2-3 x 10^5 g/mol. The desirable properties of spider silk are due to the ordered chain structure and morphology of the repeating hexapeptide sequence in the polypeptide chain, $(Gly\text{-}Ala\text{-}Gly\text{-}Ala\text{-}Gly\text{-}Ser)_n$ where

Gly, Ala and Ser are the amino acid residues glycine, alanine and serine respectively. Spider web silks are normally crystalline and highly elastic. The fibers are three to five microns in diameter, with tensile strengths in the range of 1420-1550 MPa and a percent elongation at break ranging from 16 to 30 [15].

Collagen is another important structural protein and is part of many materials in the human body. It is a repeating tripeptide involving predominantly the amino acids glycine (Gly) and proline (Pro), $(Gly\text{-}Pro\text{-}Y)_n$ where Y can be any of the other amino acids. Elastin, another useful polypeptide, is made up of various repeating structures but principally the following:

Gly-Gly-Val-Pro ; Pro-Gly-Val-Gly-Val ; Pro-Gly-Val-Gly-Val-Ala

Elastin is crosslinked via the formation of desmosine and isodesmosine units from reactions between lysine units on adjacent chains.

In work going on in England, Ashley and his group [2] have obtained silk-like structural proteins by synthetic gene expression. In this symposium, Dr. Kaplan of the Army's Natick Research Center will be presenting work accomplished on recombinant spider silk proteins for fiber production. The cloning and expression of entire genes producing polymers such as silk or spider web fibroin is labor intensive and may result in products that are difficult to isolate, purify and process into a final material. However, by producing short chain analogs, i.e. oligopeptides with the desired sequence and chain length of silk fibroin or elastin using a synthetic gene, one can have more flexibility in engineering the final product. Natural silk has only about 60% of its chain segments in ordered amino acid sequences. Thus, these oligopeptides from the spider web synthetic gene would crystallize more easily and comprise crystalline domains completely. These macromers (high molecular weight monomers) could then be linked together to prepare high molecular weight polymers with various architectures. Included are homopolymers, block copolymers (using two different oligopeptide macromers such as from spider web silk and elastin), crosslinked gels and interpenetrating networks. Joseph Cappello [2] from Protein Polymer Technologies has reported the preparation of silk-like homoblock copolymers and also alternating copolymers of various amounts of silk-like and elastin-like blocks ranging from a ratio of 1:4 to 2:1.

RESIN PRECURSORS

An important application of biotechnology is to obtain key intermediates needed for the preparation of polymeric materials. The most fascinating example is the production of poly-p-phenylene

developed by ICI [16]. Polyphenylene is an insoluble, infusable polymer with outstanding temperature resistance, low moisture absorption and a high dielectric constant. However, it is these very properties which make the polymer very difficult to produce and supply in a usable form. ICI offers a precursor that is soluble in simple organic solvents and can be readily processed into a matrix material for composite applications. A simple curing procedure converts the precursor into partially crystalline polyphenylene. The key step in the precursor synthesis (Fig. 5) is the microbial mediated synthesis of cis-1,2-dihydrocyclohexa-3,5-diene (Benzene cis glycol). This reaction step, which involves harnessing the kinetically sluggish molecular oxygen molecule for controlled and selective oxygen insertion reactions, is possible only with microbial systems.

Selective microbial hydroxylation could be used to put hydroxyl groups ortho to the amino or nitro groups on a benzene ring which would provide a simple low cost precursor to polybenzoxazole systems. Another important biosynthesis application would be the ability to obtain microbial systems capable of creating a terminal acetylene group from a precursor group such as acetyl. This would provide an improvement in cost and selectivity of state-of-the-art synthetic routes to acetylene terminated matrix resin systems (ATX).

BIOPROCESSING

Natural polymer composites as discussed in the earlier biomimetic section are intended for a specific and limited set of functions and as such find little direct use in advanced composite applications. However, the biopolymers synthesised by the various living organisms in making their composite structures possess unique functionalities and properties that qualify them as excellent candidates for creating novel synthetic/natural polymer composites. Biologically derived polymers, such as cellulose and chitin, could be used as the fiber component in thermoplastic matrix composites. They offer a substantial savings in cost with reasonable strength properties. For example, Woodhams et al [17] concluded that wood cellulose fibers possess specific strength and modulus values which compare favorably with those of glass fibers (Fig. 6). It has been shown that the use of tailor-made cellulosic graft copolymers as interfacial agents/compatibilizers improves fiber/matrix adhesion [18,19] which would further improve properties.

Biologically derived polymers could also be used as the matrix component by blending with synthetic thermoplastic components. The reactive functionality (for example the $-NH_2$ group in Chitosan) could be used to develop three dimensional crosslinks which would

confer increased strength properties. The problem in preparing such a system by mixing two incompatible polymers is that the resulting product has lower physical properties due to high interfacial tension and poor adhesion. A new technology has been developed [20,21,22] that allows the preparation of tailor-made natural/synthetic polymer graft copolymers with precise control over molecular weights, degree of substitution and backbone-graft linkage. The preparation of controlled cellulose/synthetic polymer crosslinked graft copolymer structures (i.e network structures with exactly defined chain segments between the cross-link points) have also been achieved. These graft copolymers can function effectively as compatibilizing/interfacial agents for alloying natural polymers with synthetic polymers. The compatibilizer provides for better adhesion, lower interfacial tension and finer dispersion of the non-continuous natural phase in the continuous plastic phase.

REFERENCES

1. Science, Vol. 219, 1983.

2. Materials Research Society Book of Abstracts, Fall Meeting, Nov. 27-Dec. 2, 1989, pp 595-609.

3. Bever, Michael B., ed., "Natural Composite Materials" Encyclopedia of Materials Science and Engineering , Pergamon Press, New York, 1986, pp 3128-3131.

4. Jeronimidis, George, "Engineering Aspects of Natural Composite Structures", Proceedings of BIOTECH '86, Online Publications, Pinner, UK,1986, pp 153-157.

5. Currey, John D., "Biological Composites", Handbook of Composites, Vol. 4 (A. Kelly and S. T. Mileiko, eds.), Elsevier Science Publishers B. V., 1983, pp 503-561.

6. Wainwright, S. A., et. al., Mechanical Design in Organisms, Princeton University Press, Princeton, New Jersey, 1976, pp 194-207.

7. Jeronimidis, George, "The Fracture Behaviour of Wood and the Relations Between Toughness and Morphology", The Proceedings of the Royal Society of London, B208, 1980, pp 447-460.

8. Chaplin, C. R., J. Gordon and G. Jeronimidis, United States Patent, No. 4,409,274, 1983.

9. Hepburn, H. R., "The Integument", Fundamentals of Insect Physiology (Murray S. Blum, ed.), John Wiley and Sons, 1985, pp 139-183.

10. Gunderson, S. and R. Schiavone, "The Insect Exoskeleton: A Natural Structural Composite", JOM, November 1989, pp 60-62.

11. Weiner, Stephen, "Organization of Extracellularly Mineralized Tissues: A Comparative Study of Biological Crystal Growth", Critical Reviews in Biochemistry, CRC Press, Vol. 20, No. 4, 1986, pp 365-408.

12. Katz, J. Lawrence, "The Structure and Biomechanics of Bone", The Mechanical Properties of Biological Materials (J.F.V. Vincent and J.D. Currey, eds.), Cambridge University Press, 1980, pp 137-168.

13. Currey,John D., "Shell Form and Strength", The Molusca, Academic Press, Vol. 11, 1988, pp 183-210.

14. Sarikaya, M., Gunnison, K. E., Yasrebi, M. and Aksay, I. A., "Mechanical Property-Microstructural Relationships in Abalone Shell", (in publication).

15. Handbook of Materials Science, 1974.

16. Ballard, D. H., A. Courtis, I. M. Shirley and S. C. Taylor, J. Chem. Soc., Chem. Commn., 1983, p. 954.

17. Woodhams, R. T., G. Thomas and D. K. Rodgers, Polymer Eng. Sci., Vol. 24, 1984, p. 1166.

18. Narayan, R., C. J. Biermann, M. O. Hunt and D. P. Horn, ACS Symp. Ser., Vol. 385, 1989, p. 337.

19. Narayan, Ramani, "Preparation of Bio-based Polymers for Materials Applications", Appl. Biochem. Biotech., Vol. 17, 1987, p. 7.

20. Biermann, C. J., J. B. Chung and R. Narayan, Macromolecules, Vol. 20, No. 5, 1987, pp 954-957.

21. Biermann, C. J. and R. Narayan, Polymer, Vol. 28, 1987, p. 2176.

22. U. S. Patent, No. 4,891,404, 1990.

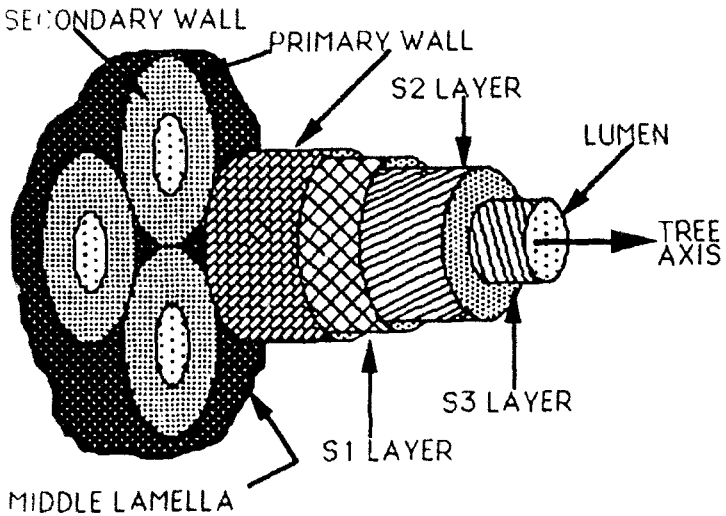

Fig. 1: General structure of the wood cell and its fiber heirarchy.

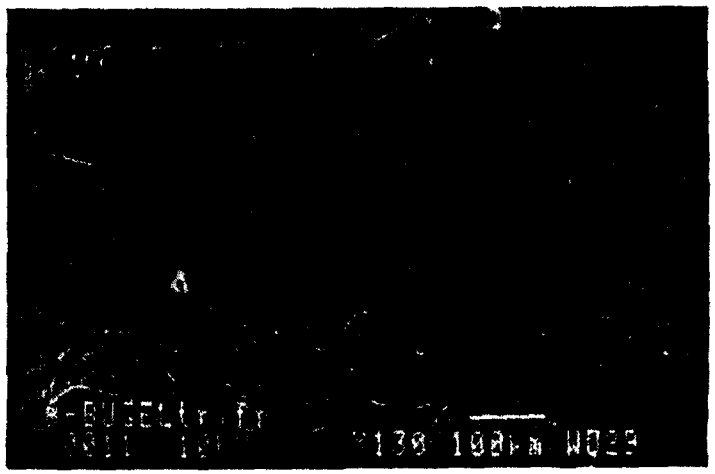

Fig. 2: SEM displaying the fibrous bessbeetle procuticle and its dual helicoid orientation.

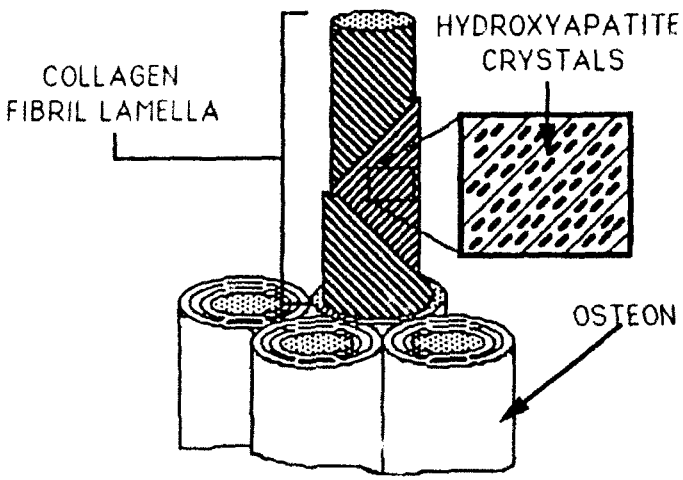

Fig. 3: Structure of the osteon from the Haversian bone system.

Fig. 4: SEM of the nacreous section in abalone shell showing its platelet lamella. (7500x)

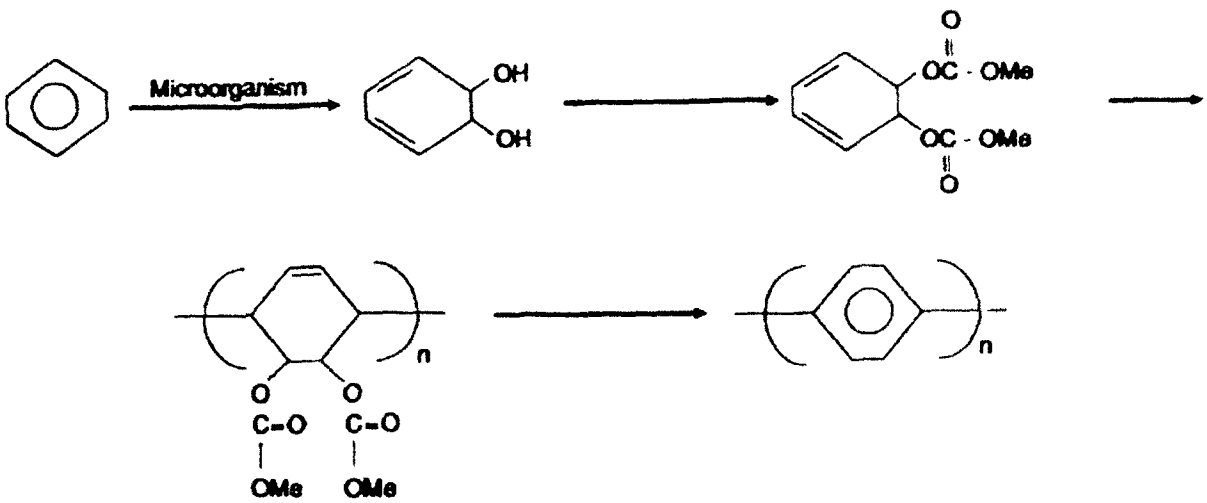

Fig. 5: Diagram of the ICI synthesis of polyphenylene through the use of microorganisms (biosynthesis).

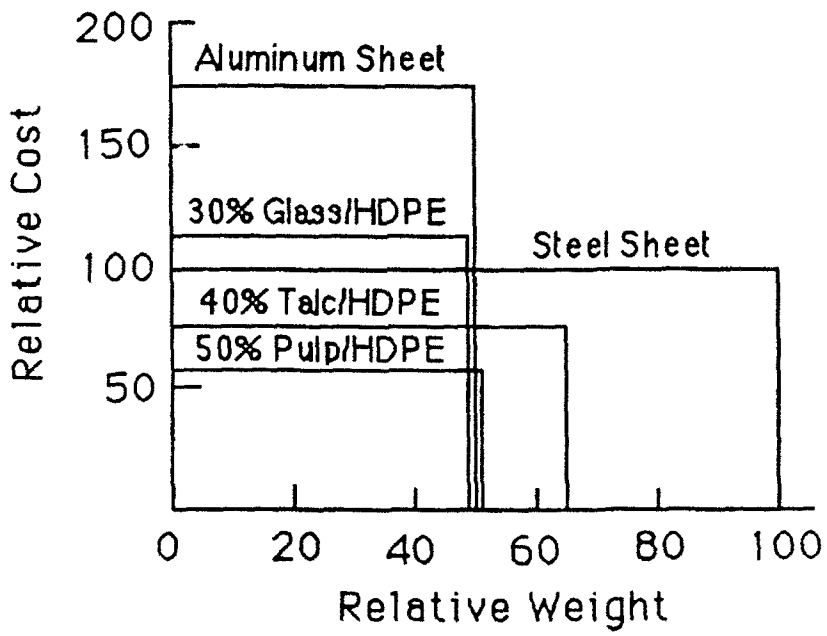

Fig. 6: Cost versus weight for materials with approximately equal stiffness.

Seashells as a Natural Model to Study Laminated Composites

M. SARIKAYA, K. E. GUNNISON, M. YASREBI, D. L. MILIUS AND I. A. AKSAY
Department of Materials Science and Engineering
Advanced Materials Technology Center
Washington Technology Centers
University of Washington
Seattle, WA 98195

1. Abstract

The microstructure and mechanical properties of the nacre section of abalone shell were studied as a model for the fabrication of laminated ceramic-metal (cermet) composites. The shell consists of laminated $CaCO_3$ (aragonite) and organic layers with thicknesses of 0.25 μm and 20 nm, respectively. The unusually high fracture toughness and fracture strength values of the shell are attributed to this unique microstructure. Laminated cermets (B_4C-Al) have been designed and processed to mimic the abalone shell. The fracture toughness and strength values of these cermets increase approximately 40% compared to the monolithic form of the same phase mixtures.

2. Introduction

In materials processing, progress is being made in controlling the microstructure of composites at the nanometer scale, resulting in the formation of materials that exhibit unprecedented mechanical, electrical, superconductive, or optical properties.[1-2] The processing of these synthetic materials is based on the additive principle, in which component phases with varying properties are fused together in an ordered manner to form a multiphase system. Conventionally, these structures can be achieved by phase transformations (precipitation-hardened alloys) or by mechanical mixtures at the microscale level (metal and ceramic matrix composites).[5] More advanced processing involves ion beam techniques (such as molecular beam epitaxy and liquid and vapor deposition)[3,4] in which the microstructure is controlled at the nanometer level. In order to meet the demands of modern technology for composites with better properties, more complex systems have to be developed through more intricate and energy-efficient processing strategies.

Methods used by living organisms in processing composites are in many ways more controlled than synthetic methods. In the formation of biological composites, living organisms can design and produce, efficiently, complex microstructures having unique properties at all spatial levels (down to the nanometer scale), and in more controlled ways at the

molecular level.[6-8] It is desirable, therefore, to produce manmade materials by using processing approaches similar to those used by living organisms, i.e., by biomimicking. This present research has been initiated to study the principles inherent in the processing methods used by organisms in producing composites and the physical properties of those composites as related to their microstructures. In this paper, we summarize the results of a recent study on the microstructures of the red abalone shell (*Haliotis rufescens*) in relation to its mechanical properties.

3. Microstructure and Properties of the Nacre Section of Abalone Shell

A longitudinal cross section of the abalone shell displays two types of microstructures: an outer prismatic layer and an inner nacreous layer. Two forms of $CaCO_3$, calcite (rhombohedral, $R\bar{3}c$) and aragonite (orthorhombic, Pmnc) constitute the inorganic component of the organic-inorganic composites in the prismatic and the nacreous layers, respectively. The structure and the properties of the nacreous layer are described here, as this is the portion of the shell which displays a good combination of mechanical properties.[9]

Mechanical properties, i.e., σ_f (fracture strength) and K_{IC} (fracture toughness), have been evaluated in the transverse direction (perpendicular) to the shell plane. Typical σ_f and K_{IC} values are 180 MPa and about 8 $MPa \cdot m^{1/2}$, respectively. The study of the crack propagation behavior reveals a high degree of tortuosity not seen in the more traditional brittle (such as Al_2O_3) and high toughness (ZrO_2) ceramics,[10] indicating that certain toughening mechanisms such as crack blunting, branching, and "layer pull-out" are operating in the shell (Figure 1). A closer examination of the microstructure reveals that cracks mostly

Figure 1. Scanning Electron Microscopy (SEM) image of multiple crack formation emanating from a microindentation.

Figure 2. High resolution SEM image of the abalone shell exhibiting the sliding of the $CaCO_3$ layers.

Figure 3. High magnification SEM image of abalone shell near a microindentation exhibiting the ligament formation of the organic phase bridging the $CaCO_3$ platelets.

advance through the organic layer and with difficulty, as this process is accompanied by sliding of the $CaCO_3$ layers (when there is a shear component of the resolved stress) and by the bridging of the organic ligaments (when there is a normal stress component), as shown in Figures 2 and 3, respectively. It is these last two mechanisms which contribute to the toughening of the shell.

The superior mechanical properties of abalone shell compared to those of more traditional ceramics and their composites (Table I) come from the unique "brick and mortar" microstructure. A Transmission Electron Microscope (TEM) image (Figure 4) recorded in the transverse direction shows the alternating layers of hexagonal-shaped 0.2-0.5 μm thick aragonite crystals which form the hard component and the thin (20-50 nm) organic substance in between (mainly proteins) which provides the ductile component of the composite.

Table I. Mechanical Properties of Ceramics, Cermets, and Abalone Shell

	σ_f MPa	K_{IC} MPa·m$^{1/2}$	Hardness	
			Mohs	KHN (kg/mm^2)
SiC	450	3.5	8.0	2750-3000
Si_3N_4	200 (SC)†	4.0	---	1500
	650 (HP)†	5.5	---	2000
ZrO_2	500	5.5	6.5	1300
Al_2O_3	270	2.0	9.0	2100
	258*	2.1*	---	---
B_4C	285	3.1-6.0	9.5	4950
$CaCO_3$	< 10	< 1.0	3.0	135
Al_2O_3-Al	500-1300	8.0	---	---
B_4C-Al	600	12.0	---	---
Abalone shell	183*	5.8*	---	240*
	(165-204)	(3.6-10.4)		

†SC - Slip Cast and HP - Hot Pressed; *this study

4. Some Microstructural Design Guidelines for Laminated Composites

The unique combination of mechanical properties of the nacre comes from both the sliding of the $CaCO_3$ layers over the organic matrix (Figure 2) and the organic ligaments that form between the layers (Figure 3). The amount of strain in sliding is as much as

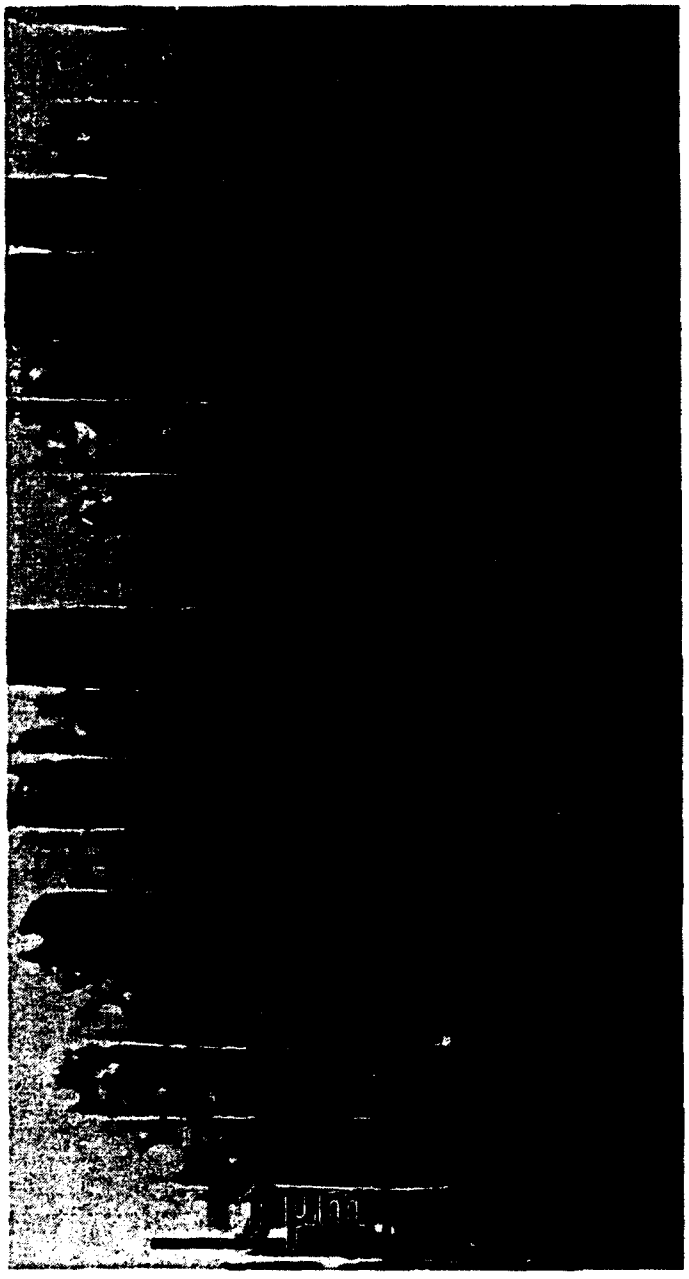

Figure 4. Bright field transmission electron microscopy image of the nacre section of the abalone shell revealing the $CaCO_3$ (C) and organic (P) layers. The image was recorded with the electron beam parallel to the laminate plane

10% without a catastrophic failure. This is similar to plastic deformation in metals caused by the gliding motion of dislocation on slip planes. Similarly, in the formation of ligaments, the organic phase elongates as much as 1000%. This is similar to superplastic deformation of metals. Both of the above processes require that the interfaces between the organic matrix and the inorganic layers do not prematurely fail. Based on these observations, the

following guidelines can be drawn for the design of laminated composites consisting of a thick, hard, and strong component and a thin, ductile, and tough component. These design guidelines are:

(i) Laminate thickness for the hard component of less than 1 μm and for the soft component of less than 100 nm;

(ii) Soft superplastic phase;

(iii) The ability of the soft phase to form ligaments;

(iv) Strong interfaces between the soft and hard layers.

In drawing these guidelines, the detailed microstructures of the soft and hard phases have yet to be taken into account. This subject will be dealt with in the future when more detailed microstructural and nanostructural information is available.

These guidelines can be followed to process laminated ceramic-metal and ceramic-polymer composites. In this section, we give some preliminary results from our ceramic-metal (cermet) research.[11] B_4C-Al is the system selected for processing the laminated cermets. By taking advantage of the limited reaction that takes place between B_4C and Al, fully dense monolithic composites with a good combination of mechanical properties have been fabricated. Figure 5 illustrates the first laminates of this cermet.[11-13] The fabrication of these

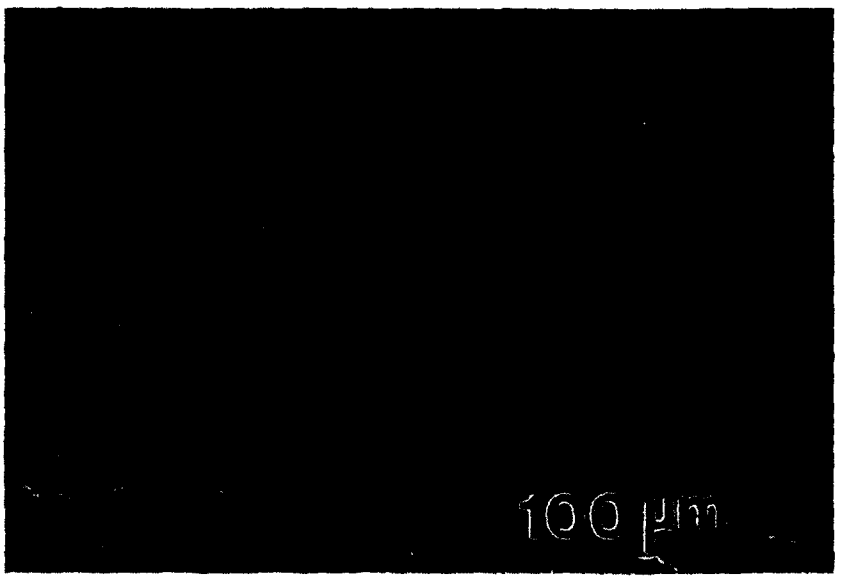

Figure 5. SEM image of B_4C-Al/Al cermet showing the fully dense microstructure.

laminates involves the infiltration of molten Al into preformed B_4C sponges of controlled porosity. The laminated composite is formed either by metal infiltration from the Al layers sandwiched between B_4C tapes or by lamination of B_4C tapes of different porosity and

then metal infiltration of the laminated body. Nearly dense laminates obtained this way show an average of 40% improvement in fracture strength (950 MPa) and fracture toughness (K_{IC}= 19 MPa·$m^{1/2}$).[11] The toughening is attributed to a similar mechanism observed in abalone shell. One of the functions of the soft phase Al, which is to "arrest" cracks, is illustrated in Figure 6 where two cracks emanating from an indentation in B_4C-Al layer

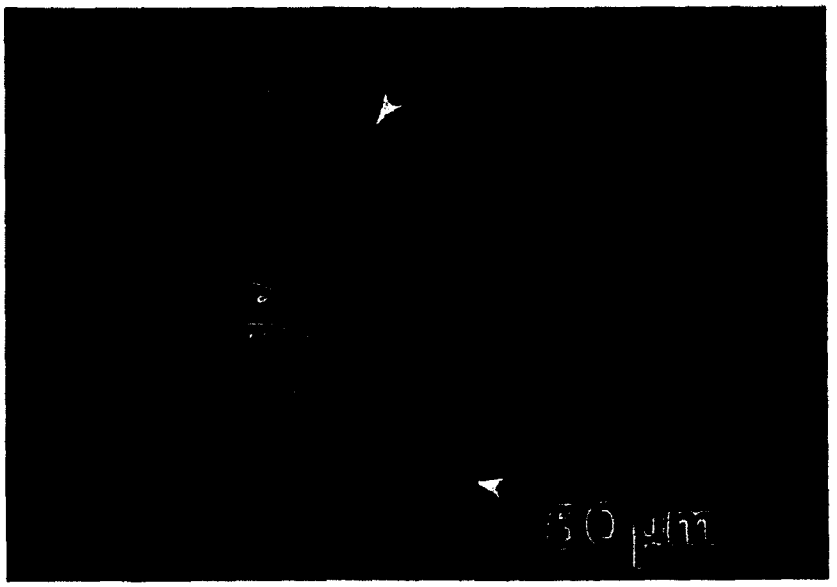

Figure 6. SEM micrographs of B_4C-Al/Al cermet revealing the effect of the soft Al layer in deflecting the microcracks (arrows) formed by a microindentation.

deviate in their normal propagation path in the vicinity of the interface. An advantage of the fabrication process described above is the ability to process graded microstructures of B_4C-Al laminates with properties that can be tailored to meet requirements which may vary along the transverse direction of the finished part, similar to abalone shell. However, in order to take full advantage of lamination in the present system, laminates of less than 10 μm thickness need to be processed. Further improvements, both in fracture toughness and strength, can be expected with decreases in the thickness of the laminates down to the submicrometer scale.

5. Summary

Preliminary results on the mechanical properties of B_4C-Al (35%) laminated cermets designed on the basis of the above observations, indicate a 40% increase in the fracture toughness and the strength of the composite. The increase in the fracture toughness is attributed to the same toughening mechanisms observed in abalone shell. Further improve-

ment in both strength and toughness is expected with the decrease in the thickness of the composite layers (to submicrometer levels); in the present case, the thinnest of the layers in the cermet laminate is about 10 μm, far too thick to benefit the effects of the lamination. Consequently, the present research is directed to the processing of cermets with submicrometer-layer thicknesses in conjunction with quantitative studies of the effects of the organic layer in seashells.

6. Acknowledgments

This research was supported by the Air Force Office of Scientific Research (AFOSR) under Grants Nos. AFOSR-87-0114 and AFOSR-89-0496.

7. References

1. Spaen, F., "The Art and Science of Microstructural Control," *Science*, **235**, 1010 (1987).
2. Cammarata, R. C., "The Supermodulus Effect in Composition Modulated Thin Films," *Scripta Metallurgica*, **20**, 883 (1980).
3. Dresselhaus, M. S., "Intercalation of Layered Materials," *Materials Research Society Bulletin*, **12** (3) 24 (1987).
4. ***Metallic Superlattices: Artificially Strong Materials***, edited by T. Sinjo and T. Takada (Elsevier, Amsterdam, 1987).
5. ***Strengthening Methods in Crystals***, edited by A. Kelly and R. B. Nicholson (Applied Science Publishers, Ltd., London, 1971).
6. Lowenstam, H. A., "Minerals Formed by Organisms," *Science*, **211**, 1126 (1981).
7. Mann, S., "Mineralization in Biological Systems," *Structure and Bonding*, **54**, 124 (1983).
8. Weiner, S., "Organization of Extracellularly Mineralized Tissues: A Comparative Study of Biological Crystal Growth," *CRC Critical Reviews in Biochemistry*, **20** (4) 365 (1986).
9. Currey, J. D., "Biological Composites," *Journal of Materials Education*, **9** (1-2) 118 (1987).
10. ***Deformation of Ceramic Materials II***, edited by R. C. Tressler and R. C. Bradt (Plenum, New York, 1984).
11. Aksay, I. A., Yasrebi, M., and Milius, D. L., "Boron Carbide-Aluminum Laminates," Invention Disclosure, submitted to Washington Technology Centers, February 14, 1990.
12. Halverson, D. C., Pyzik, A. J., Aksay, I. A., and Snowden, W. E., "Processing of Boron Carbide-Aluminum Composites," *Journal of the American Ceramic Society*, **72** (5) 775 (1989).
13. Pyzik, A. J., Aksay, I. A., and Sarikaya, M., "Microdesigning of Ceramic-Metal Composites," ***Ceramic Microstructures '86: Role of Interfaces***, edited by J. A. Pask and A. G. Evans (Plenum, New York, 1987), pp. 45.

Recombinant Spider Silk Proteins for Composite Fibers

S. J. LOMBARDI, S. FOSSEY AND D. L. KAPLAN

ABSTRACT

The use of genetic engineering for polymer synthesis provides many opportunities for control of chain composition, sequence, size, reactivity and stereochemistry. Silk proteins represent an unusual class of structural fibers with interesting mechanoelastic properties. Some types of sider silk exhibit improved mechanical properties when compared with silkworm silk. Therefore, spider silk was cloned and expressed in a bacterial host system. Research on selectively modifying composition at the genetic level to effect structural and functional changes in fiber properties is continuing. Applications in the material sciences are expected due to the versatility and properties of this class of fibers.

INTRODUCTION

Silks represent an unusual class of fibers generally considered to be protein in composition. Unlike enzymes which are termed globular proteins, silks belong to the structural fibrous protein class which also includes keratin and collagen. Silk proteins exhibit a high degree of crystallinity which is derived from the anti-parallel beta sheet secondary structure. This crystalline array is stabilized by a combination of hydrogen bonding between anti-parallel chains, and hydrophobic interactions between the sheets or layers. These interactions result in a class of fibers with unusual and interesting properties, including high tensile strength.

In addition, there is evidence for noncrystalline or amorphous regions in the secondary structure of the silk and it is believed that these regions give rise to extensibility of the fiber and the resulting property of high energy absorption to break. It is the unusal combination of high strength and high extensibility that drives much of the interest in this class of fiber.

S. J. Lombardi, S. Fossey, D. L. Kaplan, U. S. Army Natick Research, Development and Engineering Center, Natick, MA, 01760-5020

In natural systems, the two common sources of silks are the domesticated silkworm, Bombyx mori, and the orb weaving spiders. The silkworm produces one type of silk used in spinning its cocoon during one stage in its life cycle. For domestic silk production the cocoon silk is boiled to remove the soluble sticky sericin protein, and the remaining fibroin portion of the silk is then unwound and used as silk fiber. Orb weaving spiders have the capability to produce many different silks, each of which is synthesized in a separate set of secreting glands in the abdomen. In addition some of the silks, such as the dragline, are produced continuously thoughout the lifecycle of the spider. Each of the different silks exhibits different physical properties and functions. These differences are reflected in the amino acid composition of the silk. Some of the silks function in web construction/engineering, in egg cocoon structures, as adhesives, and in prey capture.

There has been some data collected on the physical properties of spider silks. Zemlin [8] and Work and Emerson [7] published data on the amino acid composition and mechanoelastic performance data of different spider silks. Dragline silk from N. clavipes has been reported to have a modulus of 1×10^{10} N/m^2, tensile strength of 1×10^9 N/m^2, and energy absorbed to break value of 1×10^5 J/kg. This compares with the silk worm which exhibits a modulus of 1×10^{10} and a tensile strength of 7.4×10^8. Both fibers exhibit about 18% elongation. Spider silks are of interest because the physical properties of the fibers appear superior to the silkworm silks.

For the silkworm, part of the fibroin gene has been mapped and partial sequencing of the 5' end of the gene was completed [2, 5, 6]. This information, in combination with X-ray data has provided the basic information on the protein structure which indicates discrete crystalline and amorphous regions as reflected in discrete coding regions in the silk gene. Genetic information on the silk worm is extensive because of the commerical interest in this material and in the translational controls over silk expression. No data on the organization of spider silk genes are available.

As in the silk worm, X-ray diffraction data on spider silk implies the presence of crystalline regions dispersed in a matrix of amorphous protein [3]. Additional data on conformation is being developed to further understand the relationships between primary and secondary structures for this class of proteins.

In addition, the capability of spiders to produce a multitude of silks with very different functions through changes in amino acid composition dictates this system as useful for genetic manipulation for fiber production. The first goal is to clone silk coding genes from the spider into a more useful expression system to increase available amounts of silk. The dragline silk, because of its high tensile strength, was chosen for cloning.

RESULTS AND DISCUSSION

To accomplish the goal of increased silk production the silk gene was cloned. First, genetic libraries were constructed from the spider. High molecular weight genomic DNA was isolated and purified from N. clavipes and then partially digested with restriction enzymes to yield 25 kb fragments. These fragments were cloned into a Lambda phage vector to generate a genomic library. RNA was purified from the major ampullate gland of the spiders. The major ampullate gland is the site of dragline silk production. The mRNA was isolated by density gradient centrifugation and oligo (dt) column chromatography and then reverse transcribed to generate a cDNA library.

To screen these libraries, the native silk protein had to be solubilized, partially hydrolyzed, and sequenced [4]. This was accomplished and the sequence data developed was used to construct DNA probes. The protein composition data confirmed the high percent of short side chain amino acids (glycine, alanine, serine) which permits the close packing density of the beta sheets. The genomic and cDNA libraries were then screened with these probes. The probes were radiolabelled by the 5' end labelling method and hybridization was determined using autoradiography. Positive clones were then subcloned and expressed in a bacterial host system. Recombinant silk protein was produced and both the clones and the silk are being analyzed. This first phase of work provides the means to produce larger quantities of silk materials for study.

The second phase of the work which is also underway involves selective modification of the natural gene sequence to tailor silk structure and properties to specific functions. To accomplish this goal, molecular modeling studies are being conducted on silk protein sequences to understand the influence of primary sequence on secondary structure. The predicted secondary structure data must then be extrapolated to predicted functional properties of the fibers spun from these sequences. This extrapolation will be validated using protein engineering techniques to enact the sequence changes in the gene, expressing the modified silk proteins, spinning fibers, and then studying fiber properties from the modified proteins.

In general, fiber spinning from recombinant silk proteins will involve mimicking the natural process used by the spider which can be correlated to spinning lyotropic liquid crystals. In the silk gland, the translated product is present in a metastable state. As the material is processed and then spun at the spinerette, there is a loss of water and the silk protein becomes highly ordered and crystalline. Physical processing appears to effect the major changes in the silk structure and there is no evidence for post-translational chemical modification of the protein. Of interest, based on the amino acid composition data collected, is the fact that spider silk fibers, despite containing a lower percentage of short side chain amino acids, exhibit superior strength properties. This would not be expected and therefore implies a significant role for the processing/spinning steps on resulting fiber properties.

Silk proteins may find application in a number of areas including composite materials. From a composites perspective, a high strength fiber such as silk with its ability to self-assemble into its secondary structure and its reactive functional groups, may provide some unique opportunities in processing and design. In addition, the environmental resistance of natural silks, presumably due to the high degree of crystallinity, would indicate that environmentally stable composite systems incorporating these materials could be considered. Illustrative of the resistance of silk fibers is the fact that proteolytic enzymes are not active in degrading silk proteins. Whether these fibers could also be incorporated into composites for biomedical implants remains to be demonstrated. Work on immobilized enzyme systems using silks for biosensor applications has already been demonstated [1].

Through genetic engineering we can now consider large scale production of fibrous proteins such as silk. The increased availability of this material will lead to many material applications in the future. In addition, the ability to tailor these structures at the genetic level to a meet specific functional requirements further amplifies the potential utility for this unusual class of fibers and for this approach to the material sciences.

REFERENCES

1. Demura, M., Asakura, T., Nakamura, E., Tamura, H., J. Biotech. 10, 113-120, 1989.
2. Gage, L. P., Manning, R. F., J. Biol. Chem. 255 (19), 9444-9450, 1980.
3. Gosline, J. M., Danny, M. W. DeMont, M. E. Nature 309, 551-552, 1984.
4. Lombardi, S. J., Kaplan, D. L., J. Arachnol. In Press.
5. Tsujimoto, Y. Suzuki, Y. Cell 16, 425-436, 1979.
6. Tsujimoto, Y., Suzuki, Y. Cell 18, 591-600, 1979.
7. Work, R. W., Emerson, P. D., J. Arachnol. 10, 1-10, 1982.
8. Zemlin, J. C. Technical Report 69-29-CM, AD684333, U. S. Army Natick Laboratories, Natick, MA, 1968.

Treatment of Graphite Fiber Surfaces with Gram-Negative Aerobic Bacteria

J. PENDRYS, A. CRASTO, R. SCHIAVONE AND S. GUNDERSON

ABSTRACT

Microorganisms perpetually seek out the organic elements C, H, N, O, S, and P, which are incorporated into their structure. Carbon and hydrogen are also oxidized to provide the energy required to sustain life. Graphite is composed of a single element - carbon, and graphite fibers contain greater than 99% carbon. Untreated graphite fibers bond poorly to polymer matrices, resulting in composites with weak shear, transverse, and off-axis properties. Fiber treatments which increase the surface functionality improve the interfacial bond. It is of interest to determine if bacteria, lacking an alternative carbon source, can utilize the carbon in graphite fibers, and chemically alter the fiber surface. In this study, various graphite fibers were exposed to two strains of gram-negative bacteria, *Pseudomonas aeruginosa* NAV6 and *Acinetobacter calcoaceticus* NAV2. Some fibers showed organic deposits attached to the surface, and are being examined further for changes in surface morphology and functionality. Changes in fiber-matrix adhesion are assessed from tests on single-fiber composites.

INTRODUCTION

Microorganisms require the organic elements C, O, H, N, S and P to multiply and survive. Carbon and hydrogen are also oxidized to provide energy for catabolism. The most commonly metabolized compounds are hydrocarbons. These organic elements are usually bound covalently to other elements, and only oxygen is routinely utilized as a pure element. Graphite fibers are composed of elemental carbon bound covalently in a graphitic structure. If bacteria can utilize elemental carbon, then they may also be able to alter the surface of a graphite fiber. In addition, bacteria routinely excrete compounds which enable them to bind to hydrophobic surfaces.

Graphite fibers, in general, have poor adhesion to polymer matrices, resulting in poor shear, transverse, and off-axis properties in the corresponding composites. Consequently, these fibers are routinely surface-treated, sized, or both prior to incorporation in a polymer matrix. Graphite fibers are composed of crystallites in which parallel graphitic basal planes are in a turbostratic arrangement, aligned along the fiber axis. The order, size, and alignment of

---

John Pendrys, Biophysicist, Biotechnology Laboratory, Naval Surface Warfare Center, Silver Spring, MD., and
Allan Crasto, Materials Scientist, Rebecca Schiavone, Biomaterials Scientist, and Stephen Gunderson, Biomaterials Technician, University of Dayton Research Institute, Dayton, OH.

these crystallites increase with increasing modulus. The edges of these basal planes contain defects, and are active sites for chemical modification. As the fiber modulus increases, the fraction of the fiber surface occupied by these edge sites decreases, making the fiber lessreactive to conventional surface treatments. Consequently, the newer, higher modulus graphite fibers display relatively poor interfacial adhesion in polymer composites.

In this study, graphite fibers were exposed to pure bacterial cultures, to determine if the fiber surfaces could indeed be altered by the bacteria. The treated fibers are being examined analytically to detect both physical and chemical changes of the surface, and mechanically characterized to monitor changes in strength and modulus as a result of the treatment. Adhesion to an epoxy matrix will be assessed by a single-fiber composite technique. If successful in promoting fiber-matrix adhesion, such bacterial treatments could provide an inexpensive, novel means of fiber surface modification.

MATERIALS

Fibers

Preliminary studies were performed on Union Carbide's unsized, pitch-based P-55 graphite fiber (modulus 55 Msi), obtained from Ron Lee of the Naval Surface Warfare Center (NSWC) [1]. Detailed investigations were conducted on sized and unsized variants of a pitch-based graphite fiber from DuPont (E-75, modulus 75 Msi) and on PAN-based AU4 and AS4 carbon fibers from Hercules Inc. The 'U' and 'S' in the latter fibers denote untreated and surface-treated fibers respectively, with the AS4 fiber being sized as well.

Media and Buffers

Distilled water was prepared with a Corning Mega-Pure Still, and deionized water (resistivity 18.1 megohm-cm) with a Nanopure II water deionization system. Distilled water has a lower concentration of organic matter than deionized water, but a higher concentration of metallic ions. Common salts and ethanol were purchased from the J. T. Baker Chemical Company, and nutrient broth was obtained from Difco Laboratories of Detroit, MI.

Minimal salts buffer (MSB) was prepared by adding the following chemicals to distilled or deionized water: K_2HPO_4, 7 g; KH_2PO_4, 3 g; $MgSO_4$, 0.1 g; $(NH_4)_2SO_4$, 1 g; and NaCl, 1 g. This is a phosphate buffer with a pH of 7.0, and no carbon source. A carbon-rich medium was prepared using nutrient broth. Minimal carbon buffer (MCB) was prepared by adding 0.5 ml of nutrient broth to 125 ml of MSB. Media and buffers were sterilized by autoclaving prior to use.

Bacterial Strains

The two bacterial strains used in this study are *Acinetobacter calcoaceticus* NAV2 and *Pseudomonas aeruginosa* NAV6. These two strains were isolated from a mixed culture of asphalt-degrading bacteria that was obtained from soil at NSWC [2]. Each strain is capable of growing rapidly on hydrocarbon sources such as hexadecane, lubricating oil, and paraffin.

METHODS

Bacterial Treatment

Preliminary studies: 5 mm lengths of sterile P-55 graphite fibers were added to 15 mm x 125 mm Kimex test tubes containing 5 ml of sterile MSB (prepared with distilled water). One test tube was inoculated with *A. calcoaceticus* NAV2, another with *P. aeruginosa* NAV6. The initial inoculum level was approximately 1×10^6 bacteria/ml. Sterile tubes containing MSB

and P-55 fibers were also prepared. All tubes were sealed for 117 days at ambient temperature with neoprene "00" stoppers. At the end of this exposure period, the fibers were washed with deionized water, ethanol, and acetone, and dried in air.

Detailed studies: Longer lengths of E-75 (sized and unsized), AU4 and AS4 fibers were placed in sterile 18 oz Nasco Whirl-Pak bags or 250 ml Nalge screw-capped bottles. Approximately 125 ml of MSB, MCB, or nutrient broth was added to each sample. Some samples were inoculated with either *A. calcoaceticus* NAV2 or *P. aeruginosa* NAV6, the inoculum level being about 1 x 10^6 bacteria/ml. Samples in sterile, uninoculated nutrient broth were contained in the bottles, while all others were prepared in the Whirl-Pak bags. Samples in MSB and MCB remained sealed at ambient temperature for 31 days; those in nutrient broth for 27 days. At the end of the exposure period, fibers from MSB and MCB were washed thoroughly with deionized water. Samples from the nutrient broth were washed with deionized water and ethanol. Twenty-six fiber samples were so treated, and the details are shown in Table 1.

Fiber Surface Characterization

Treated fiber surfaces were examined in a scanning electron microscope (SEM) from AMRAY Inc., to detect any physical evidence of bacterial attack. Deposits on the fiber surface were analyzed by energy dispersive x-ray analysis (EDAX) on equipment procured from EDAX International. Any chemical changes on the fiber surface were monitored by x-ray photoelectron spectroscopy (XPS).

Fiber Property Characterization

Changes in fiber strength are determined by tensile tests on individual fibers in an Instron, using a 50 g load cell. The influence of the bacterial treatment on the adhesion of the fiber to polymer matrices is determined from interfacial shear strength (IFSS) measurements on single-fiber composites. In this test, an epoxy coupon (Epon 828 cured with 14.5 phr m-phenylenediamine) containing a single embedded (aligned) fiber is stressed in tension. The fiber breaks sequentially at a number of points, and stress is applied until no more breaks are observed, while the specimen itself is still intact. Using a differential equation for the force balance of an elastic fiber embedded in a plastic matrix, the IFSS, τ, is related to the fiber diameter, d, and strength, σ_f, and the ultimate (critical) fiber length, l_c, through the expression [3]:

$$l_c/d = \sigma_f/2\tau$$

In practice, the specimen is stressed under a microscope, and the fiber fractures are easily observed in-situ with polarized light, according to a technique developed by Drzal, et al. [4]. The parameter l_c is therefore conveniently measured without the necessity of extracting the fiber fragments. Fiber strength (σ_f) and diameter (d) are measured in a separate test. The parameters l_c and σ_f are not constant, but statistically distributed. These distributions have been combined by a statistical theory [5] to yield a statistical distribution for τ.

RESULTS AND DISCUSSION

After four months of exposure to the bacteria, the P-55 fibers from the initial studies were examined by SEM. Phosphate crystals had precipitated out of all the buffers, and all fibers displayed some erosion at the ends (Figures 1 and 2). The fibers in the sterile MSB appeared clean and unaffected by their exposure to the buffer, while those in buffer inoculated with bacteria were heavily fouled with phosphate crystals. An EDAX examination of these crystals found them to contain mainly elements from the MSB. The elements Fe, Ni and Cr were also detected in the crystals. These are the elements of stainless steel, and probably arise from metallic impurities in the water. The bacteria are clearly responsible for binding

these hydrophilic, ionic crystals to hydrophobic, covalent graphite. In addition, the crystals were attached to the graphite fiber surfaces in an aqueous environment. These P-55 fibers are approximately 10 microns in diameter. As bacteria are approximately one to two microns in diameter, any bacteria attached to the fiber surface should be readily detected. However, no bacteria were observed. If there had been any attached earlier, they were probably removed during the washing process.

From the studies on E-75, AU4 and AS4 fibers, at the end of the exposure period, only sample 15 (AS4 fiber in MSB inoculated with NAV2) had non-graphitic material attached to the fiber surface (Figure 3). SEM and EDAX examinations revealed this to be fibrous, organic matter. This material held the fibers together, and appeared to be weaker than its adhesive bond to the fibers. This fibrous matter is probably a lipopolysacharride, which is commonly excreted by gram-negative bacteria. A few bacteria were also visible at the ends of this fibrous material. Since these fibers were sized, it is possible that the bacteria utilized the organic sizing and not the fiber itself. This is being investigated further. No crystals precipitated out of solution, or were found attached to the fibers. It is possible that the metallic ion concentration in the deionized water used to prepare the buffer was too low for crystals to precipitate. SEM examinations of other fiber samples revealed no visible evidence of biodegradation, and XPS will be used to detect any changes in surface functionality. IFSS measurements will quantify the effect of the exposure on the adhesion of these fibers to an epoxy matrix.

ACKNOWLEDGMENTS

We thank Marriner Norr for performing the SEM and EDAX studies. This research was supported in part by the Naval Surface Warfare Center as part of its basic research program, and under U. S. Air Force contract F33615-87-C-5239.

REFERENCES

1. F. Santiago, A. N. Monsour and R. N. Lee, Surf. and Interf. Anal, 10, (1987) pp. 17-22.

2. J. P. Pendrys, Appl. and Environmental Technol., 55, (1989) pp. 1357-62.

3. A. Kelly and W. R. Tyson, J. Mech. Phys. Solids, 13, (1965) p 329.

4. L. T. Drzal, et al., 35th Ann. Tech. Conf., SPI, RP/C Institute, (1980) Secn. 20-C.

5. A. S. Crasto, S. H. Own and R. V. Subramanian, Polym. Compos., 9(1), (1988) pp. 78-92.

TABLE 1. Preparation of graphite fiber samples

Sample Number	Fiber	Sizing	Buffer/ Medium	Bacterial strain	Exposure time (days)
-	P-55	N	MSB	Sterile	117
-	P-55	N	MSB	NAV2	117
-	P-55	N	MSB	NAV6	117
1	E-75	Y	MSB	Sterile	31
2	E-75	Y	MSB	NAV2	31
3	E-75	Y	MSB	NAV6	31
4	E-75	Y	Nutrient	Sterile	27
5	E-75	Y	Nutrient	NAV2	27
6	E-75	Y	Nutrient	NAV6	27
7	E-75	N	MSB	Sterile	31
8	E-75	N	MSB	NAV2	31
9	E-75	N	MSB	NAV6	31
10	E-75	N	Nutrient	Sterile	27
11	E-75	N	Nutrient	NAV2	27
12	E-75	N	Nutrient	NAV6	27
13	E-75	N	MCB	NAV6	31
14	AS4	Y	MSB	Sterile	31
15	AS4	Y	MSB	NAV2	31
16	AS4	Y	MSB	NAV6	31
17	AS4	Y	Nutrient	Sterile	27
18	AS4	Y	Nutrient	NAV2	27
19	AS4	Y	Nutrient	NAV6	27
20	AU4	N	MSB	Sterile	31
21	AU4	N	MSB	NAV2	31
22	AU4	N	MSB	NAV6	31
23	AU4	N	Nutrient	Sterile	27
24	AU4	N	Nutrient	NAV2	27
25	AU4	N	Nutrient	NAV6	27
26	AU4	N	MCB	NAV2	31

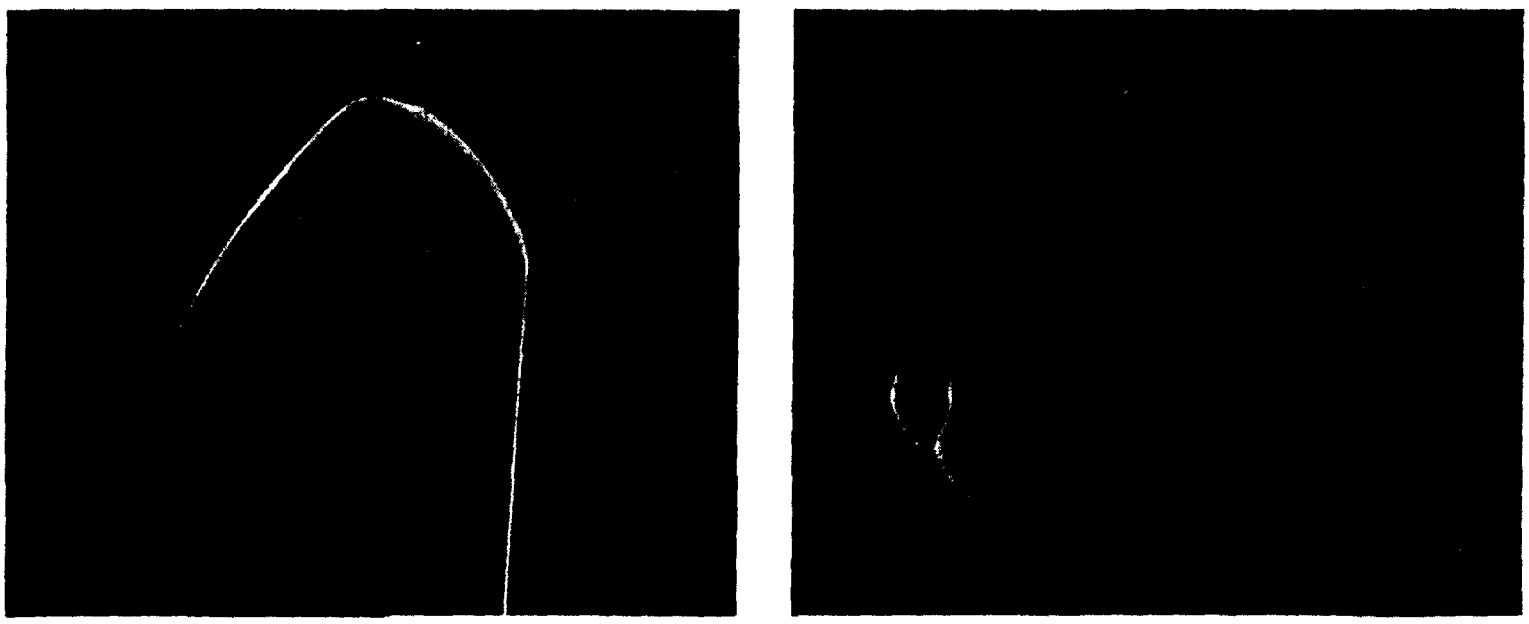

5000 X

2000 X

FIGURE 1. Scanning electron micrographs of P-55 graphite fibers exposed to sterile MSB for 117 days

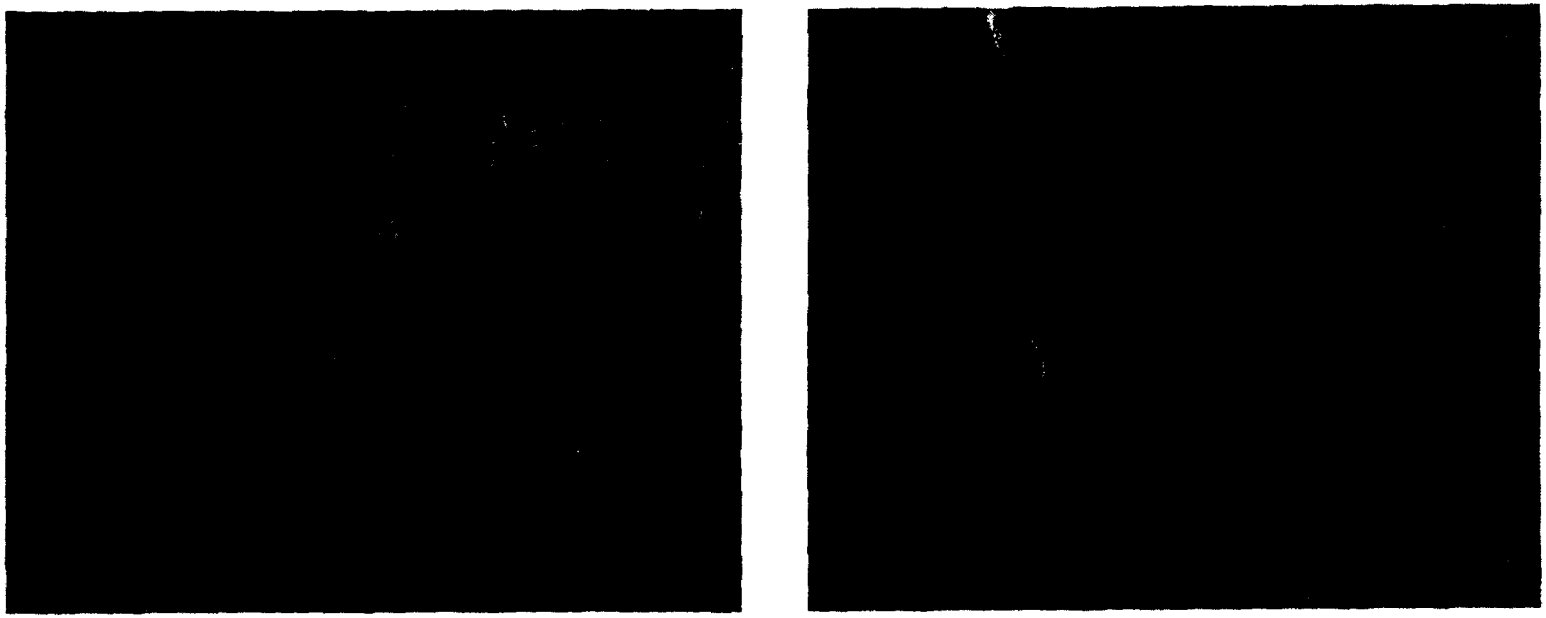

5000 X

2000 X

FIGURE 2. Scanning electron micrographs of P-55 graphite fibers exposed for 117 days to MSB inoculated with (A) *P. aeruginosa* NAV6, and (B) *A. calcoaceticus* NAV2

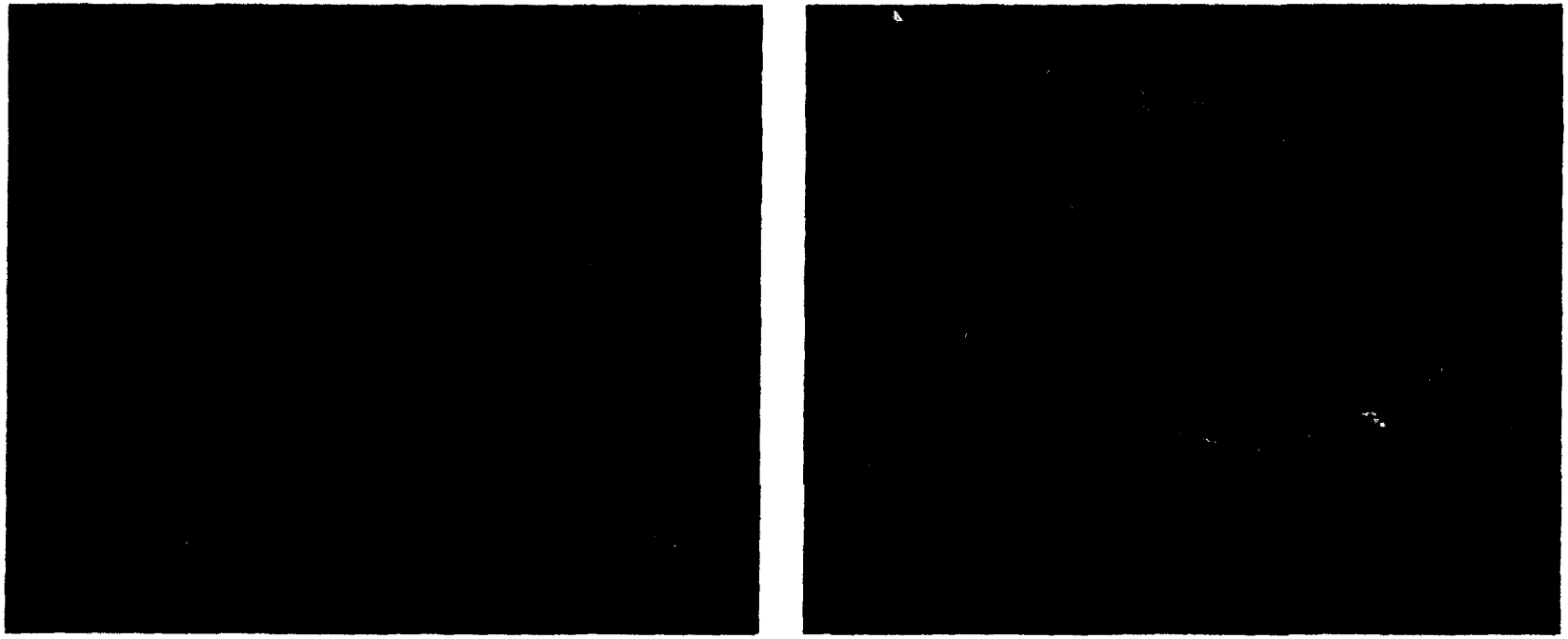

FIGURE 3. Scanning electron micrographs of AS4 graphite fibers exposed for 31 days to MSB inoculated with *A. calcoaceticus* NAV2.

Modeling the Effects of Aging on Bone Properties Using Composite Material Micromechanics

H. A. HOGAN

ABSTRACT

A two-dimensional finite element quarter-fiber micromechanics model for compact bone has been developed and used to study the effects of aging on mechanical properties. Aging generally increases the porosity of compact bone due to larger Haversian canals, which are the hollow centers of osteons. A three-component micromechanics model has been developed with the elastic modulus of the osteon (hollow fiber) being 12.0GPA and the interstitial bone tissue (matrix material) being a slightly stiffer 15.0GPa. Poisson's ratio has been taken to be 0.30 in both cases. The amorphous material surrounding each osteon is called the cement line and is widely regarded to be much more compliant than the bone components. Thus, the cement line (interphase material) modulus is 6.0GPa and Poisson's ratio 0.40. Longitudinal and transverse moduli for 0, 3, 5, 7, and 9 percent porosities are presented. They are generally lower than experimental data and not as sensitive t changes in porosity as some have observed. Finite element solutions also reveal the detailed variations in "micro-level" stresses throughout the microstructure for a given average macroscopic applied stress. These localized stress concentrations and their changes with age are important parameters in the continuing pursuit of a more deterministic understanding of the way bone responds and adapts to mechanical stimuli.

INTRODUCTION

Compact bone tissue, also known as cortical bone, is the dense highly mineralized bone material that forms the mid-shaft of major long bones such as the femur, tibia, and humerus. A thin protective layer of compact bone also covers the spongy, or trabecular, bone that forms the bulbous processes at the ends of such bones. In mature compact bone the main microstructural element is the Haversian system, or secondary osteon. Thus, this bone is sometimes referred to as osteonal bone or Haversian bone. A secondary osteon is roughly cylindrical in shape, has a hollow center, and is aligned parallel to the major axis of long bones. Osteons are sheathed by thin layers of amorphous material and packed together similar to a fiber reinforced composite material. In this case, the matrix material is interstitial bone tissue, which is similar in

Department of Mechanical Engineering, Texas A & M University, College Station, TX 77843-3123

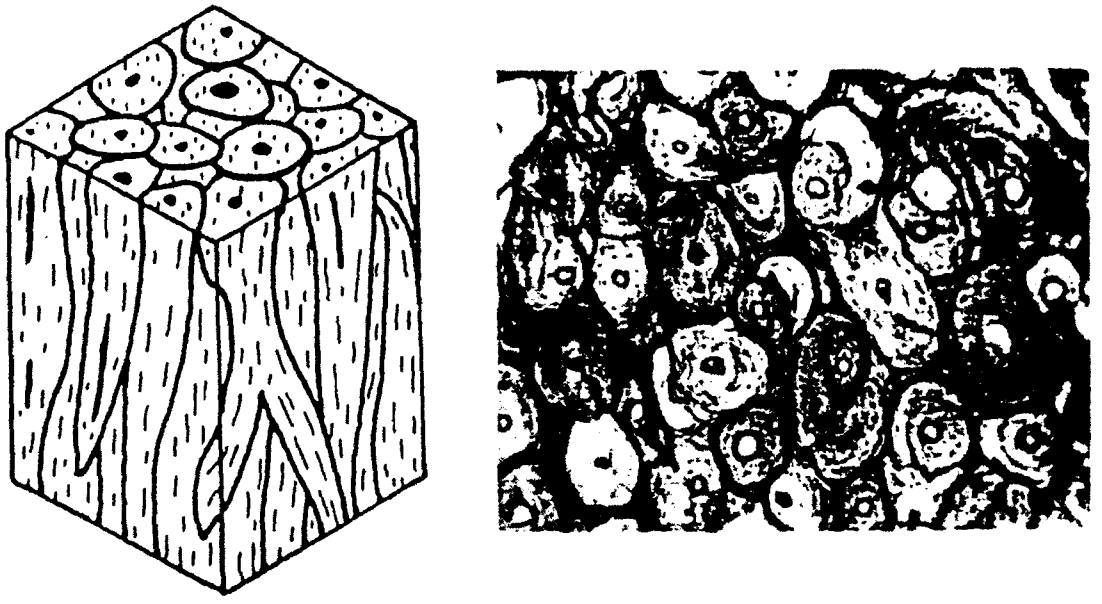

(a.) (b.)

Fig. 1. Haversian bone microstructure.
(a.) schematic depiction (after Currey [1])
(b.) photomicrograph (after Martin & Burr [2])

composition to osteons but less organized. A three-dimensional perspective view and a cross-sectional view of Haversian bone are presented in Figure 1.

Currey's early work [3] represents the first significant formal attempt to analyze compact bone as a composite material. A two-component model was used in this work, with compact bone treated simply as a mixture of collagen and minerals. Currey later [4] extended his work by treating the two-phase model more specifically as a fiber reinforced composite. With this approach the mineral crystals are considered to be relatively stiff fibers that are reinforced by a more compliant matrix of collagen. Piekarski [5] followed a similar approach and also introduced a "hybrid" model, which was an adaptation of a model for reinforced concrete.

Perhaps the most elegant model to date is the hierarchical model proposed by Katz [6,7]. On the "ultrastructural" level, lamellar bone tissue, which is laid down in concentric layers to form osteons, is treated much like the fiber reinforced composite of Piekarski, in which case the elastic modulus and Poisson's ratio of lamellar bone are expressed in terms of its collagen and mineral constituents. The angular orientation of the collagen fibers and mineral crystals are included in this analysis. On a higher level, the "microstructural" level, Haversian compact bone tissue is treated as a fiber reinforced composite material with secondary osteons forming the fibers, which are embedded in a matrix comprised of cement lines, interstitial lamellae, and minerals. This matrix is referred to collectively as an amorphous "binder" material. Osteon fibers are assumed to be arranged in a regular hexagonal array. Upper and lower bound solutions for this arrangement have been established

by Hashin and Rosen [8], and have been used to obtain solutions for compact bone. The model has been applied inversely to infer estimated properties of compact bone constituents (Katz, et al. [9]).

The application of finite element analysis to micromechanics modeling greatly enhances its power and usefulness by providing exact solutions rather than only upper or lower bounds as is the case with the analytical models reviewed above. Adams and co-workers [10,11] have been particularly productive in developing such methods for studying fiber reinforced composites. Two salient features of finite element micromechanics models are that they allow the quantitative characterization of: (1) the effects of constituent properties and arrangement on macroscopic behavior, and (2) the distribution of stresses and strains amongst tissue constituents. In applying such techniques to bone tissue, the first feature would allow the modeling of microstructural changes as a result of disease or simply the aging process. Porosity, the orientation of collagen fibers in lamellar bone layers, and the degree of mineralization of bone tissue are all known to change with age [12]. The second feature mentioned, the ability to model "microlevel" stresses and strains, would provide important new information to complement continuing efforts by both engineering and medical researchers to quantify and understand bone remodeling and adaptation [1,13-15]. In many of these works, connections are sought between mechanical loads, the macroscopic stresses and strains that they generate in bone, and subsequent bone remodeling activity. With micromechanics modeling, more direct relationships could be investigated, i.e. the relationship between stresses and strains in bone constituents and associated remodeling. The effects of aging (resulting from changes in porosity and lamellar bone collagen fiber directions) on these processes could also be evaluated.

MICROMECHANICS MODELING

The current work is an attempt to apply micromechanics modeling techniques for continuous fiber reinforced aerospace composites to modeling compact bone tissue. Specifically, the WYO2D finite element computer code developed by Adams and co-workers has been modified and adapted to incorporate bone tissue features. In this effort, fiber spacing is assumed to be in a regular square array, such that only a quarter-fiber and its surrounding matrix material need be modeled. The two-dimensional grid of triangular, 3-noded elements used for modeling a transverse section of material is shown in Figure 2. The main contributor to compact bone porosity is assumed to be the Haversian canal, which is included in the model by treating the fiber as hollow. The fiber volume percent is 70% and the porosity for the case shown is 9%. The model also contains a separate interphase layer of material between the fiber and matrix. In this case, this is intended to represent the "cement line" material. The mechanical properties of each of these three components are as follows:

E_f=12GPa & ν_f=0.3 for osteons (fiber component)
E_m=15GPa & ν_m=0.3 for interstitial bone (matrix component)
E_c=6GPa & ν_c=0.4 for cement lines (interphase component).

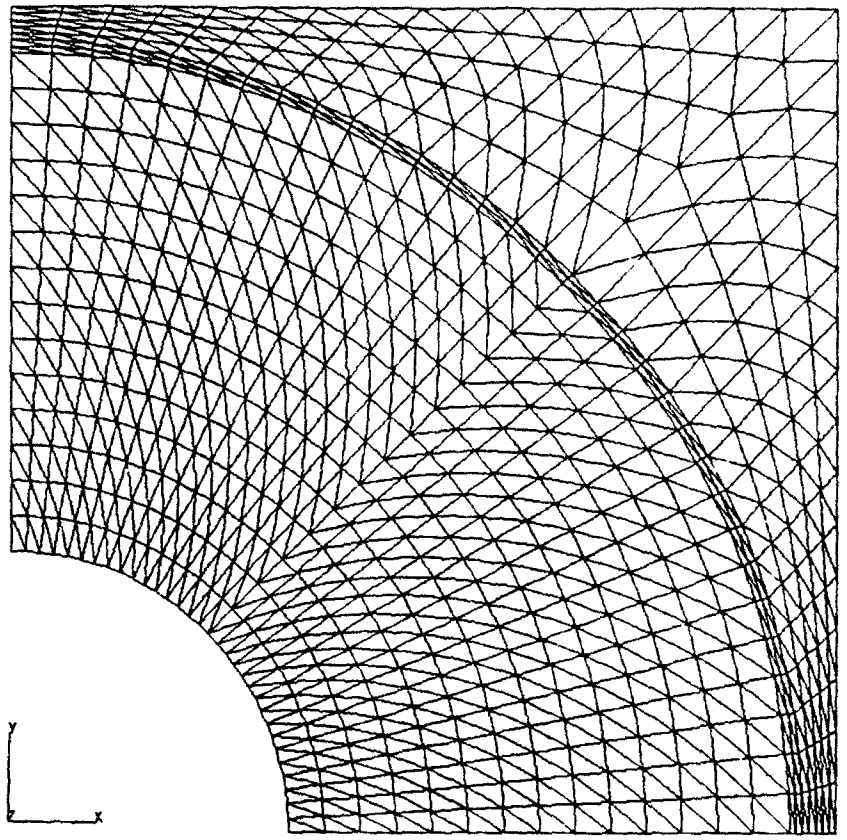

Fig. 2. Micromechanics model.

The value for the elastic modulus (E_f) of osteons is the maximum reported by Ascenzi and Bonucci [16] for single osteons in tension, while that for interstitial lamellae (E_m) has been taken to be slightly higher than that for osteons as suggested by Evans and Vincentelli [17]. Proper values for cement lines are not clear. Some contend that this material is stiffer than bone tissue [1], while most [18-20] consider it to be more compliant. The properties used here are twice as compliant as bone.

RESULTS AND DISCUSSION

Finite element solutions have been obtained for two homogeneous macroscopic stress states: (1) a longitudinal normal stress (parallel to fibers) of σ_z=15MPa, and (2) a transverse normal stress of σ_x=15MPa. These loads are applied in the computer program such that the surfaces or boundaries of the unit cell remain parallel to their original orientation during deformation. This prevents the formation of any voids or gaps in the model. Using the overall strain in the direction of the applied stress permits calculation of macroscopic elastic moduli as summarized in Table I. Results are also included from earlier studies of a two-component quarter-fiber micromechanics model for compact bone tissue [21]. The range of experimental values reported by Van Buskirk and Ashman [22] for wet human compact bone are presented as well.

Table I

Macroscopic Elastic Modulus

	Porosity	E_z (GPa)	E_x (GPa)
3-Component Model hollow fiber	0	12.7	12.5
	3	12.3	11.7
	5	12.1	11.1
	7	11.9	10.6
	9	11.6	10.1
2-Component Model solid fiber	0	21.8	12.6
Experimental [22]	?	17.0-21.5	6.9-14.4

The predicted properties for the transverse modulus, E_x, are well within the experimental range, but the values for the longitudinal modulus, E_z, are much lower. The two-component model results generally agree well and this is not surprising since the component properties that were used in this case were taken from a study of Katz, et. al [9], in which properties were inferred from experimental data for macroscopic properties. The analytical model used in this work treated the osteons as the fiber component (solid) and the cement line and interstitial bone material together as an equivalent "binder" matrix material. Thus, the following properties were used for the two-component finite element micromechanics model:

E_f=30.0GPa & ν_f=0.30 for osteons (fiber)
E_b=2.77GPa & ν_b=0.27 for the binder (matrix)

It should also be pointed out that the analysis from which these values come was based upon an assumed regular hexagonal spacing for the fibers and a fiber volume percent of 92%.

The consistently lower values of E_z are a direct result of trying to use fiber properties from experimental data on individual osteons. Obviously, the macroscopic moduli cannot be any higher than the stiffest component. Beginning with an osteon modulus of 12.0GPa and using 15.0GPa for the interstitial lamellar bone, as suggested by Evans and Vincentelli [17], forces the overall macroscopic modulus to be lower than experimentally observed values. If the three-component model is to be a valid model, then the fiber modulus should probably be higher, as was the case with the two-component model. Recent experimental work on "microspecimens" (less than 500μm thick) of compact bone show a size dependence in properties, with a general trend toward lower strengths and moduli as the specimen size decreases [23]. An explanation put forth for this behavior is that at smaller sizes secondary vascular channels become more significant because their relative size increases. These channels typically run radially from the Haversian canal to the cement line and are

frequently considered to be only minor contributors to compact bone porosity. They very well may, however, explain the lower modulus values reported for single osteons. Including these features in the micromechanics model is an issue for further research. Using a higher fiber modulus would require re-examination of the observations of Evans and Vincentelli [17]. Their work was based upon correlations of properties determined from "macrospecimens" with microstructural characteristics such as percent Haversian area and lamellar bone collagen fiber orientation. Re-evaluating these results in light of recent observations from tests on microspecimens seems warranted.

The variation in properties with porosity shows the expected trend of decreasing stiffness with increasing porosity. Schaffler and Burr [24] have tested 3mm diameter bovine bone samples and correlated properties with porosity, bone volume fraction (1-porosity), ash content, and apparent. They found the strongest correlation ($r=0.84$) to be a power law expression relating modulus (longitudinal only) to bone volume fraction. The predicted modulus (E_z) values for 3, 5, 7, and 9 percent porosities are 24.3, 19.4, 15.3, and 12.1, respectively (all in GPa). The results from the present work are again generally lower, but also exhibit much less sensitivity to porosity. Secondary vascular channels may again offer an explanation. Martin and Ishida [25] report correlations between tensile strength for bovine bone and eight different microstructural and compositional parameters. Several different bone types were studied and for the osteonal bone, porosity was calculated from both Haversian canals and secondary vascular channels (Volkmann's canals). Data from 13 specimens gave an average total porosity of 6.8% with the Haversian porosity component being only 2.8%. This provides further motivation for including Volkmann's canals in the micromechanics model, as has already been mentioned. The first option being considered for doing this is to treat the solid part of the hollow osteon as an anisotropic material with different properties in the longitudinal and transverse directions. Modeling the osteon structure with discrete concentric layers of lamellar bone would accomplish this objective while also providing a means of including collagen fiber orientation in the model. Each layer of lamellar bone would have different properties in the longitudinal direction as well as in the radial and tangential directions in the transverse plane. Another possible way to improve the model would be to create a 3-dimensional unit cell, which would include regularly spaced voids in the longitudinal direction.

Detailed "micro-level" stress distributions for the 9% porosity case are given in Figures 3-5. These results are all for the same homogeneous macroscopic applied stress of σ_x=15MPa. Considering Figure 3, note that σ_x varies within the microstructure from a high of 44.2MPa to a low of -.629MPa. The plot also shows that both the maximum and minimum values occur at the inner surface of the Haversian canal. This kind of information is particularly significant since the bone cells that play a major role in bone remodeling and adaptation are located primarily on this surface. This surface not only sees stresses much higher and lower than the average macroscopic value, but it also sees large stress gradients. Some stress concentration is also present in the cement line interphase region near the top of the model where σ_x is in the mid 20's. Figures 4 and 5 show significant "induced" stresses in the microstructure even

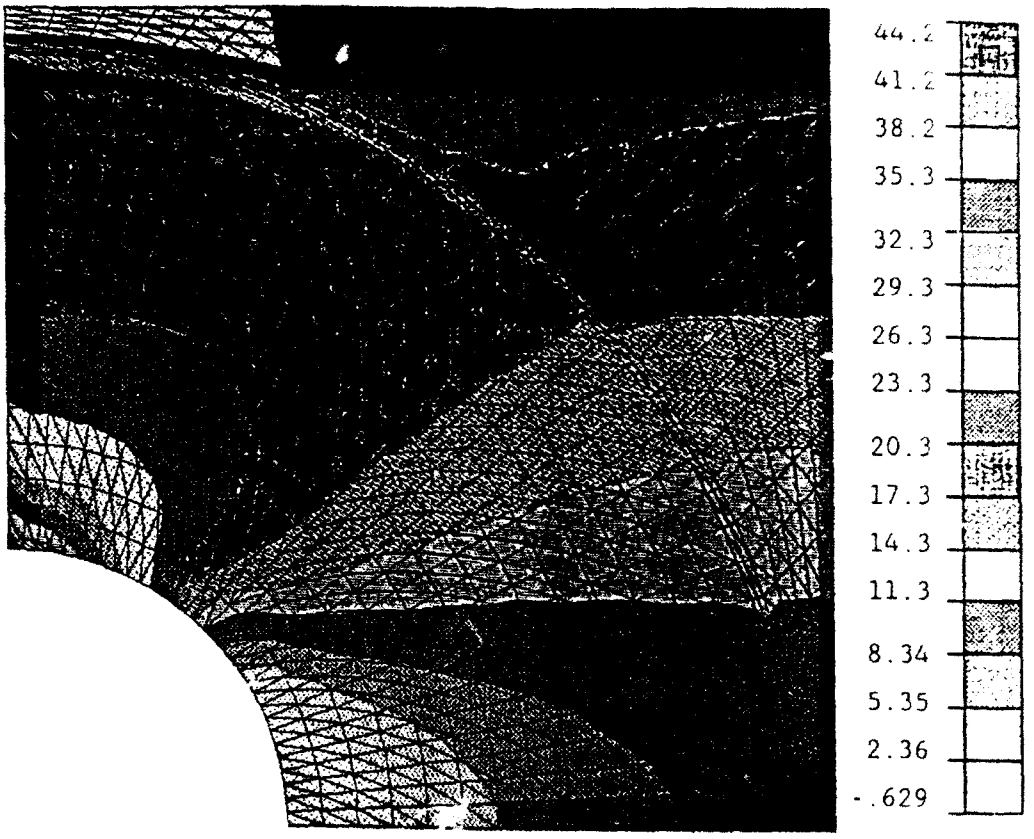

Fig. 3. Distribution of σ_x for a macroscopic average applied stress of σ_x=15.0MPa.

though both σ_y and τ_{xy} are zero macroscopically. Extreme values and large gradients again tend to occur along the surface of the Haversian canal and in the interphase region.

The results presented herein demonstrate clearly the power and potential usefulness of a micromechanics model for compact bone tissue. The major challenge is in developing and properly verifying a valid and clinically relevant model. The specific improvements needed are indeed formidable, but not by any means unattainable. The knowledge gained from this process will also shed considerable light on the very complex relationships between structure, form, and function in this highly efficient and amazingly adaptive "natural" or "biological" composite material. The insights and principles elucidated could very well form an important contribution to the continuing pursuit of more advanced and effective "man-made" composite materials.

REFERENCES

1. Currey, J. (1984) The Mechanical Adaptations of Bones. Princeton University Press, New York.
2. Martin, R. B. and Burr, D. B. (1989) Structure, Function, and Adaptaion of Compact Bone. Raven Press, New York.
3. Currey, J. D. (1964) Three analogies to explain the mechanical properties of bone. Biorheology 2, 1-10.

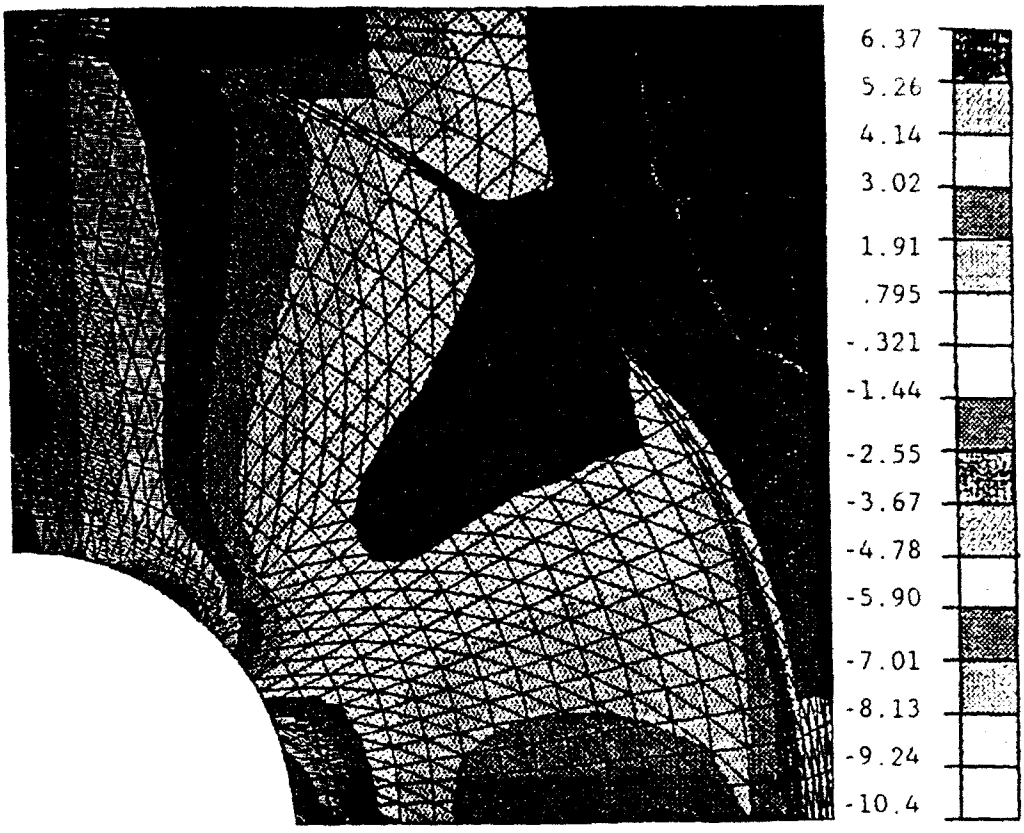

Fig. 4. Distribution of σ_y for a macroscopic average applied stress of σ_x=15.0MPa.

4. Currey, J. D. (1969) The relationship between the stiffness and the mineral content of bone. J. Biomech. **2**, 477-480.
5. Piekarski, K. (1973) Analysis of bone as a composite material. Int. J. Eng. Sci. **10**, 557-565.
6. Katz, J. L. (1976) Hierarchical modeling of compact haversion bone as a fiber reinforced material. Advances in Bioengineering. (edited by Mates, R. E. and Smith, C. R.) pp. 17-18. American Society of Mechanical Engineers, New York.
7. Katz, J. L. (1981) Composite material models for cortical bone. Mechanical Properties of Bone (edited by Cowin, S. C.) AMD Vol. 45, pp. 171-184. American Society of Mechanical Engineers, New York.
8. Hashin, Z. and Rosen, B. W. (1964) The elastic moduli of fiber reinforced materials. J. Appl. Mech. **31**, 223-232.
9. Katz, J. L., Yoon, H. S., and Maharidge, R. L. (1985) The estimation of inter-osteonal mechanical properties from a composite model for haversian bone. Biomechanics: Current Interdisciplinary Research. (edited by Perren, S. M. and Schneider, E.) pp. 179-184. Martinus Nijhoff, Dordrecht.
10. Adams, D. F. (1974) Elastoplastic crack propagation in a transversely loaded unidirectional composite. J. Comp. Matl. **8**, 38-54.
11. Adams, D. F. and Crane, D. A. (1984b) Combined loading micromechanical analysis of a unidirectional composite. Composites **15**, 181-191.

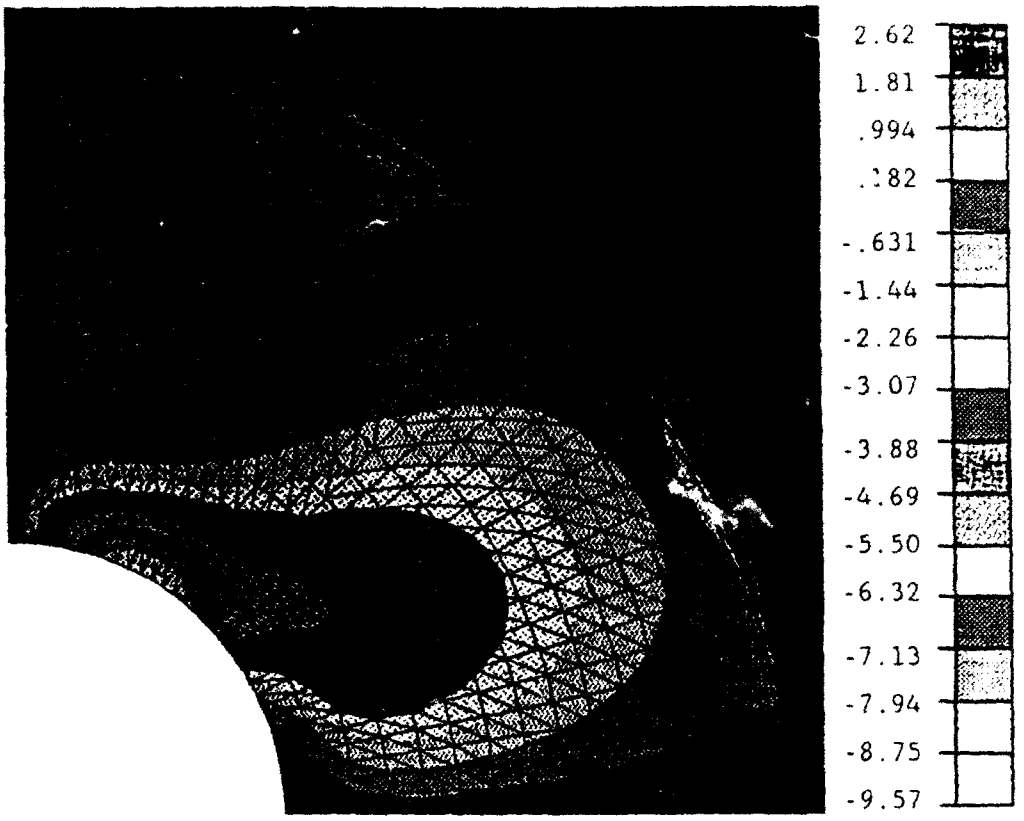

Fig. 5. Distribution of τ_{xy} for a macroscopic average applied stress of σ_x=15.0MPa.

12. Simmons, D. J. (1985) Options for bone aging with the microscope. Yearbook of Physical Anthropology. **28**, 249-263.
13. Carter, D. R. and Wong, M. (1988) Mechanical stresses and endochondral ossification in the chondroepiphysis. J. Orthop. Res. **6**. 148-154.
14. Cowin, S. C. (1987) Bone remodiling of diaphyseal surfaces by torsional loads: theoretical predictions. J. Biomech. **20**, 1111-1120.
15. Rubin, C. T. and Lanyon, L. E. (1987) Osteoregulatory nature of mechanical stimuli: function as a determinant for adaptive remodeling in bone.
16. Ascenzi, A. and Bonucci, E. (1967) The tensile properties of single osteons. Anat. Rec. **158**, 375-386.
17. Evans, F. G. and Vincentelli, R. (1974) Relations of the compressive properties of human cortical bone to histological structure and calcification. J. Biomech. **7**, 1-10.
18. Lakes, R. and Saha, S. (1979) Cement line motion in bone. Science **204**, 501-503.
19. Frasca, P., Harper, R., and Katz, J. L. (1981) Strain and frequency dependence of shear storage modulus for human single osteons and cortical bone microsamples - size and hydration effects. J. Biomech **14**, 679-690.

20. Schaffler, M. B., Burr, D. B., and Frederickson, R. G. (1987) Morphology of the osteonal cement line in human bone. Anat. Rec. 217, 223-228.
21. Hogan, H. A. (1989) Composite material micromechanics modeling of Haversian bone. 1989 Biomechanics Symposium. (edited by Torzilli, P.A. and Friedman, M.H.) AMD Vol. 98, pp. 161-164. American Society of Mechanical Engineers, New York.
22. Van Buskirk, W. C. and Ashman, R. B. (1981) The elastic moduli of bone. Mechanical Properties of Bone (edited by Cowin, S. C.) AMD Vol. 45, pp. 131-143. American Society of Mechanical Engineers, New York.
23. Choi, K., Kuhn, J. L., Ciarelli, M. J., and Goldstein, S.A., (1989) The elastic modulus of trabecular, subchondral, and cortical bone tissue. 1989 Biomechanics Symposium. (edited by Torzilli, P.A. and Friedman, M.H.) AMD Vol. 98, pp. 165-168. American Society of Mechanical Engineers, New York.
24. Schaffler, M. B., Burr, D. B., and Frederickson, R. G. (1987) Morphology of the osteonal cement line in human bone. Anat. Rec. 217, 223-228.
25. Martin, R. B. and Ishida, J. (1989) The relative effects of collagen fiber orientation, porosity, density, and mineralization on bone strength. J. Biomech. 22, 419-426.